BONE MICROSTRUCTURE EVALUATION NEAR UNLOADED DENTAL IMPLANTS COMBINING CONFOCAL SCANNING LASER MICROSCOPY, CIRCULARLY POLARIZED LIGHT MICROSCOPY, AND SEM BACKSCATTERED ELECTRONS IMAGING

T. TRAINI, M. DEGIDI[1], G. MURMURA, A. PIATTELLI and S. CAPUTI

Department of Stomatology and Oral Sciences, School of Dentistry, University "G. d'Annunzio", Chieti; [1]Private practice Bologna, Italy

The aim of this report is to present a new investigative approach to implant dentistry based on the correlation of qualitative and quantitative data reported on the same figure by overlapping different images collected on the specimen with different investigative systems. Six unloaded titanium dental implants retrieved with peri-implant bone from the mandible of 2 patients after a 6 month period were used in this study. Samples of the peri-implant tissues embedded in resin were imaged by scanning electron microscopy using backscattered electrons signal (SEM BSE), confocal scanning laser microscopy (CSLM) and circularly polarized light microscopy (CPLM). The SEM BSE images were used to identify the different levels of mineral density. The CSLM images provided all the information on cells and bone marrow spaces. The CPLM images gave the collagen fibre orientation. To overlap the images we used a program introduced by Alan Boyde, based on a linear transformation matrix which projects one system onto the other. The total bone area investigated was of $695x10^3$ pixels. The low mineral density index was 40.1, with an extension area of $344x10^3 \pm 23x10^3$ pixels (mean ± SD) while the high mineral density index was 54.8 with an extension area of $317x10^3 \pm 22x10^3$ pixels (mean ± SD). Transverse collagen fibers showed an extension area of $201x10^3 \pm 25x10^2$ pixels (mean ± SD) (28.9%), while the area for longitudinal orientation was $282x10^3 \pm 19x10^2$ pixels (mean ± SD) (40.6%). The marrow spaces showed an extension of $113x10^3 \pm 24x10^2$ pixels (mean ± SD) (16.3%). This method demonstrated that bone near unloaded implants showed almost the same extension for longitudinal and transverse collagen fibre with a predominantly low mineral density index closest to the implant surface.

In implant dentistry, the processing of samples which include tissues and metals uses a cutting-grinding technique, first described by Donath et al (1). With this method, nevertheless, it is almost impossible to obtain serial sections of the same specimen for different investigations, due both to the limited number of sections that can be prepared and the large quantity of specimen that is lost during the cutting-grinding procedures. We believe that a combined analysis using different procedures such as scanning electron microscopy with backscattered electrons (SEM BSE), Confocal Scanning Laser Microscopy (CSLM), Circularly Polarized Light microscopy (CPLM) could improve the quality of the results; Moreover, it is certainly valuable to correlate information obtained under different investigations by exactly overlapping two or more images giving the opportunity to overcome the limitations of each investigation system. Under CPLM microscopy we can obtain data pertaining to the different collagen orientation in the peri-implant bone (2), while using SEM BSE signal we can have information about the mineral content of the bone (3). Compositional (atomic number contrast) mode BSE SEM of plastic embedded specimens in implant dentistry was considered useful in demonstrating differences of bone mineral density at sub-micron resolution (4-7). Sample preparation technique is critical and requires that superficial topographic relief is minimal; nevertheless, it must be considered that polishing leads to the development of relief related to the changes in collagen orientation in bone lamellae, due to related changes in micro hardness and polishing wear resistance (8). Confocal Scanning Laser Microscopy (CSLM) gives an improved opportunity to study blocks of hard tissues. Excellent structural information can be obtained in the reflection mode, by the use of a laser. There is usually sufficient auto-fluorescence signal in bone tissue to read general histology and identify cell types and matrix structure. Nevertheless, if this is not enough, the fluorescent signal can be improved by staining with basic fuchsin in ethanol solution (0.1%). The best way to obtain several strongly fluorescent areas remains (when possible) intra-vital administration of fluorescent dyes (9-12), that labels the bone mineralisation front (13).

The present study aims to evaluate the human bone

Key Words: bone, block microscopy, Circularly Polarized Light Microscopy, Confocal Laser Scanning Microscopy, overlapping, osteoid, osteocytes, scanning electron microscopy

Mailing address:
Dr. Tonino Traini DDS, PhD
Department of Stomatology and Oral Sciences,
Via dei Vestini 31,
66100 Chieti, Italy
Fax: ++39 0871 3554072
e-mail address: t.traini@unich.it

0394-6320 (2007)

microstructure near unloaded dental implants using a new investigation approach based on the correlation of qualitative and quantitative details by overlapping BSE SEM, CSLM and CPLM images.

MATERIALS AND METHODS

Specimen preparation. Six unloaded titanium dental implants (XiVE plus, DENTSPLY-Friadent, Mannheim, Germany) retrieved with peri-implant bone from the mandible of 6 patients after a 6 month period were used in the present study. Written, informed consent to participate in the study, which was approved by the local Ethics Committee, was obtained for all patients. The specimens were dehydrated in ethanol series and embedded in LR White resin (London Resin, Berkshire, UK). Six non decalcified cut sections were prepared by means of TT System (TMA2, Grottammare, Italy) and ground to a final thickness of 100 μm ± 5 μm (mean ± SD) using a graded series (240 to 1.200) of silicone carbide grit papers under running water. The remaining blocks were finished and lapped using 0.5 μm – 0.3 μm and finally 0.1 μm diamond powder.

Image acquisition. For CSLM, a Zeiss Axiovert 200 M with the LSM 510META scanning module (Carl Zeiss, Jena, Germany) equipped with three lasers HeNe (543 nm, 1 mW) HeNe (633 nm, 5 mW) and Ar (458- 477- 488- 514 nm, 30 mW) was used. The micro milled block surface was coupled to a cover slip using glycerine (which is easily removed by washing with distilled water). All the images were collected using a high-NA C-APOCHROMAT dry objective (40/1.2) at 12 bit (MxN 1024 x 768 grid of pixel) with line average technique. For SEM, a LEO 435 Vp was used (LEO Electron Microscopy Ltd, Cambridge, UK) with an automated digital SEM with tetra solid-state BSE detector. SEM operating conditions included 30-KV accelerating voltage, 15 mm working distance, 1.2 nA probe current. The images (MxN 1024x 768 grid of pixel) were captured in an external control computer using a line average technique. Standardisation of the BSE signal was achieved by use of brominated and iodinated dimethacrylate resin standards as described by Howell et al. (14) and Boyde et al. (7). Samples were coated with gold by vacuum evaporation Emitech K 550 (Emitech Ltd, Ashford, Kent, UK). Au-sputtering was used rather than C-sputtering since it is more easily controlled and is reported as a useful method (15). For CPLM, an Axiolab light microscope (Carl Zeiss, Jena, Germany), equipped with two linear polarizers and two quarter wave plates arranged to have a transmitted circularly polarized light, was used. The microscope was connected to a digital camera (FinePix S2 pro, Fuji Photo co. LTD, Minato-ku, Tokyo, Japan) controlled by a software package with image capturing capabilities (FinePix Hyper-Utility 2, Fuji Photo co. LTD, Minato-ku, Tokyo, Japan). The digitized images were stored in format TIF with NxM = 1024 x 788 grid of pixels. Collagen fibers aligned perfectly transverse to the direction of the light propagation (parallel to the plane of the section) appeared "white-blue" due to a change in the refraction of exiting light whereas the collagen fibers or crystals aligned along the axis of light propagation (perpendicular to the plane of the section) appeared "red-yellow", because no refraction occurred.

The software package. The software package tailored to the overlapping needs by Boyde et al. (16) was used. This program uses a linear transformation matrix which projects one system onto the other by finding three corresponding points in the two pictures (Fig. 1), following the equation (1)

$$\vec{X}^1 = A\vec{X}^2 + \vec{B}$$

Where $\vec{X}^1$s the position of a point in the first image, $\vec{X}^2$is the position of the corresponding point in the second image, A is the transformation matrix with the following elements:

$$A = \begin{pmatrix} a & b \\ c & d \end{pmatrix}$$

and $\vec{B}$ is the translation vector of the system as following:

$$\vec{B} = \begin{pmatrix} e \\ f \end{pmatrix}$$

The software functions by finding three corresponding pairs of points resulting in six coordinates for the image translation. The transformation matrix and translation vector were funded by solving the equation (2) for six unknowns:

$$\begin{aligned} x_1 &= ax_1^1 + by_1^1 + e \\ y_1 &= cx_1^1 + dy_1^1 + f \\ x_2 &= ax_2^1 + by_2^1 + e \\ y_2 &= cx_2^1 + dy_2^1 + f \\ x_3 &= ax_3^1 + by_3^1 + e \\ y_3 &= cx_3^1 + dy_3^1 + f \end{aligned}$$

Where pixels were not used, adjacent points were linearly interpolated. The centres of the coordinated systems were the central pixels in each image (Fig. 1).

Special procedure. The mineralization index was evaluated using two different grey levels forming the Region of Interest (ROI). Low Mineral Density Index (LMDI) and High Mineral Density Index (HMDI) were both evaluated using the following equation (3):

$$_{L-H}MDI = \sum_{i=i}^{k} \frac{A_i \times \bar{X}GL}{A_t}$$

where A_i was the bone area of interest with grey levels comprised between i to k, $\bar{X}GL$ was the mean of the grey level considered in the area of interest, while A_t was the total area of the image occupied by bone tissue without considering marrow spaces and osteocyte lacunae.

RESULTS

The investigated peri-implant bone area was composed of 695 x10^3 ± 19 x10^2 pixels (mean ± SD). The mineral density indexes, calculated using equation (3) was 40.1, with an extension area of 344 x10^3 ± 23 x10^3 pixels (mean ± SD) and a grey level mean of 81 for the low value; while, for the high value was 54.8 with an extension area of 317 x10^3 ± 22 x10^3 pixels (mean ± SD) and a grey level mean of 120 (Fig. 2). The investigation

Table I. *Summary of the data collected.*

Mineral Density Index		Collagen Fibers Orientation		Marrow Spaces
Low	High	Transverse	Longitudinal	
40.1	**54.8**	**28.9%**	**40.6%**	**16.3%**

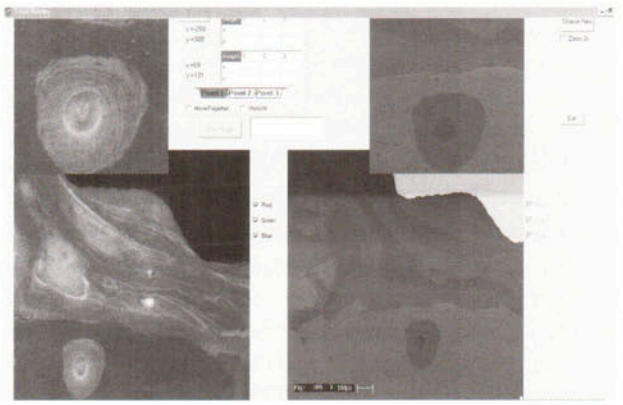

Fig. 1. *Bone tissue around unloaded dental implant after 6 months. Screen capture at step 1, finding the corresponding CSLM (left) and BSE-SEM (right) images. In the left image the light-grey is due to tissue auto fluorescence, while the medium-grey within bone domain is due to acid fuchsine stain. In the right image, within bone domain, the high mineral density areas appear whiter. Field width of SEM image = 2300μm.*

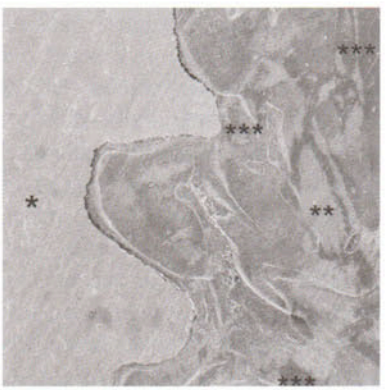

Fig. 3. *Combine SEM BSE and CPLM images for collagen fiber orientation. (*) the titanium implant. (**) transverse collagen fibers orientation. (***) longitudinal collagen fibers orientation.*

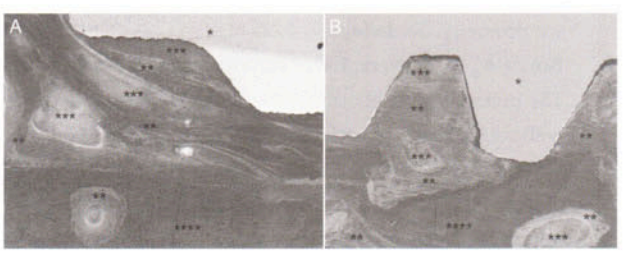

Fig. 2. *A and B combine SEM BSE and CSLM images of peri-implant bone for mineral density index. (*) the titanium implant. (**) newly formed bone mainly formed by low-mineralised bone matrix with (***) marrow spaces inside the tissue. (****) Highly mineralized bone matrix. Field width = 560μm.*

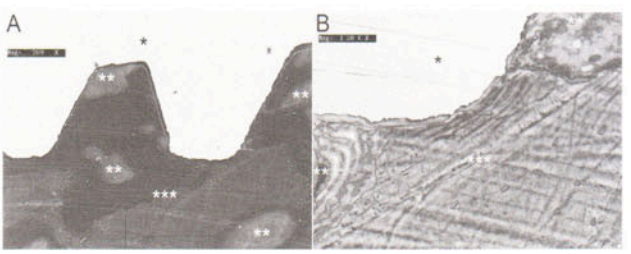

Fig. 4. *A and B combine SEM BSE and CSLM images for marrow spaces. (*) the titanium implant. (**) marrow spaces. (***) bone tissue.*

on collagen fibers showed an extension area of 201 $x10^3$ ± 25 $x10^2$ pixels (mean ± SD) for transversely oriented collagen fibers (28.9%), while the area occupied by longitudinally oriented collagen fibers was 282 $x10^3$ ± 19 $x10^2$ pixels (mean ± SD) (40.6%) (Fig. 3). The marrow spaces occupied 113 $x10^3$ ± 24 $x10^2$ pixels (mean ± SD) (16.3%) (Fig. 4). All data was summarized in Table I .

DISCUSSION

Bone is a hierarchically structured material with remarkable mechanical performance. Understanding its microstructure is essential for the assessment of the physiological response to load. The amount of mineral is usually thought to determine the stiffness of the bone; nevertheless, the properties of the organic matrix as well as the geometrical arrangement of the two components might have a much larger influence. This collagen-mineral composite contains nano-sized mineral particles (essentially carbonated hydroxyapatite), proteins (predominantly collagen type I), and water. These components have extremely different mechanical properties: the elasticity of bone and thus its resistance to fracture is related to its degree of mineralization,

because an increase in stiffness and brittleness of bone tissue follows the replacement of its water content by mineral. The (wet) protein is much softer but also much tougher than the mineral one. Remarkably, the composite combines the optimal properties of the components, such as stiffness and toughness. This rather unusual combination of the property of the material provides both rigidity and resistance against fracture. From the viewpoint of clinical implication, a better understanding of the bone microstructure around unloaded dental implants might help to define in a better way the loading clinical protocol for delayed loaded implants. The method presented here enables the overlapping of images obtained under BSE SEM, CSLM and CPLM; these techniques give information on the mineral density, marrow spaces and collagen fiber orientation of the peri-implant bone tissues respectively. The images had using CSLM present an enhanced depth of focus field (17) and this is especially useful for the study of the cells and soft tissues, while, on the other hand, SEM BSE imaging is excellent in obtaining information on mineral density.

Howell and Boyde (8) reported that the information depth in 20kV BSE SEM imaging of bone is of the order of one μm, with most signals deriving within the top half μm. CPLM investigation is of interest due to the birefringence of the bone tissue that gives the opportunity to correlate the clinical application of dental implants (under occlusal loading or unloading) to the bone matrix organization with a very time efficient technique (2,18-9). Collagen fibres have been implicated in the initiation of matrix calcification with the involvement of many other matrix proteins including chondrocalcin, proteoglycans, osteonectin, and osteocalcin (20). The results of this study agree with one of our previously published studies in humans, where a prevalent longitudinally collagen fibre orientation near unloaded implants was reported (2).

The present technique provides a new approach for combining structures visible only under a specific investigation system in an image of predetermined size, facilitating in general the specimen analysis. This method may be useful to investigators who use a variety of complex imaging systems.

In conclusion the method presented, for the cross-comparison of SEM BSE, CSLM and CPLM of the same layer in the surface of a flat block of tissue, demonstrates that bone near unloaded implants showed almost the same extension for longitudinal and transverse collagen fibers with a predominantly low mineral index with a rate of 16.3% of marrow spaces closest to the implant surface.

ACKOWLEDGEMENTS

We are grateful to Prof. Alan Boyde for his help and assistance for providing the software used in this study. This work was partially supported by the National Research Council (C.N.R.), Rome, Italy, by the Ministry of Education, University, Research (M.I.U.R.), Rome, Italy.

REFERENCES

1. **Donath K. and G. Breuner.** 1982. A method for the study of undercalcified bones and teeth with attached soft tissue *J. Oral Pathol. 11:318.*
2. **Traini T., M. Degidi, S. Caputi, R. Strocchi, D. Di Iorio and A. Piattelli.** 2005. Collagen fiber orientation in human peri-implant bone of immediately loaded and unloaded titanium dental implants. *J. Periodontol. 76:83.*
3. **Goldman H.M., A. Blayvas, A. Boyde, P.G.T. Howell, J.G. Clement and T.G. Bromage** 2000. Correlative Light and Backscattered Electron Microscopy of Human Bone. Part II: Automated Image Analysis. *Scanning 22: 337.*
4. **Boyde A. and S.J. Jones.** 1983. Backscattered electron imaging of skeletal tissues. *Metab. Bone Dis. Rel. Res. 5:145.*
5. **Roschger P., H. Plenk Jr, K. Klaushofer and J. Eschberger.** 1995. A new scanning electron microscopy approach to the quantification of bone mineral distribution: backscattered electron image grey-levels correlated to calcium Kalpha-line intensities. *Scanning Microscopy 9:75.*
6. **Vajda E.G., J.G. Skedros and R.D. Bloebaum.** 1998. Errors in quantitative backscattered electron analysis of bone standardized by energy-dispersive X-ray spectrometry. *Scanning 20:527.*
7. **Boyde A., R. Travers, F.H. Glorieux and S.J. Jones.** 1999. The mineralisation density of iliac crest bone from children with osteogenesis imperfecta. *Calci. Tiss. Int. 64:185.*
8. **Howell P.G.T. and A. Boyde.** 1999. Surface roughness of preparations for backscattered electron scanning electron microscopy: the image differences and their Monte Carlo simulation. *Scanning 21:361.*
9. **Frost H.M.** 1962. Tetracycline labelling of bone and the zone of demarcation of osteoid seams. *Can. J. Biochem. Physiol. 40:485.*
10. **Hulth A. and S. Olerud.** 1962. Tetracycline labelling of growing bone. *Acta Soc. Med. Upssala 67:219.*
11. **Rahn B.A. and S.M. Perren.** 1970. Calcein blue as a fluorescent label in bone. *Experientia 26:519.*
12. **Rahn B.A. and S.M. Perren.** 1971. Xylenol orange, a fluorochrome useful in polychrome sequential labelling of calcifying tissues. *Stain Technol. 46:125.*
13. **Boyde A.** 1987. Applications of Tandem scanning Reflected Light microscopy and 3-dimensional imaging. *Ann. N. Y. Acad. Sci. 483:428.*
14. **Howell P.G.T., K.W.M. Davy and A. Boyde.** 1998. Mean atomic number and backscattered electron coefficient calculations for some materials with low mean atomic

number. *Scanning 20:35.*

15. **Bloebaum R.D., J.G. Skedros, E.J. Vajada, K.N. Bachus and B.R. Constantz.** 1997. Determining mineral content variations in bone using backscattered electron imaging. *Bone 20:485.*
16. **Boyde A., L. Lovicar and J. Zamecnik.** 2005. Combining Confocal and BSE SEM imaging for bone block surfaces. *European Cells and Materials 9:33.*
17. **Boyde A. and S.J. Jones.** 1995. Mapping and measuring surfaces using reflection confocal microscopy. In: *Handbook of Biological Confocal Microscopy, 2nd edition*, J.B. Pawley ed. Plenum Press. New York, p. 255.
18. **Traini T., M. Degidi, R. Strocchi, S. Caputi and A. Piattelli.** 2005. Collagen fibers orientation near dental implants in human bone: do their organization reflect differences in loading? *J. Biomed. Mater. Res. 74:538.*
19. **Traini T., S. De Paoli, S. Caputi, G. Iezzi and A. Piattelli.** 2006. Collagen fibers orientation near a fractured dental implant after 5-year loading period: case report. *Implant Dent. 1:70.*
20. **Farquharson C., B.H. Thorp, C.C. Whitehead and N. Loveridge.** 1994. Alterations in glycosaminoglycan content and sulfation during chondrocyte maturation. *Calcif. Tissue Int. 54:296.*